

# Analytic solution of the SEIR epidemic model via asymptotic approximant

Steven J. Weinstein,<sup>1,2</sup> Morgan S. Holland,<sup>1</sup> Kelly E. Rogers,<sup>1</sup> and Nathaniel S. Barlow<sup>1, a)</sup>

<sup>1)</sup>*School of Mathematical Sciences, Rochester Institute of Technology, Rochester, NY 14623, USA*

<sup>2)</sup>*Department of Chemical Engineering, Rochester Institute of Technology, Rochester, NY 14623, USA*

(Dated: 22 November 2022)

An analytic solution is obtained to the SEIR Epidemic Model. The solution is created by constructing a single second-order nonlinear differential equation in  $\ln S$  and analytically continuing its divergent power series solution such that it matches the correct long-time exponential damping of the epidemic model. This is achieved through an asymptotic approximant (Barlow et. al, 2017, Q. Jl Mech. Appl. Math, 70 (1), 21-48) in the form of a modified symmetric Padé approximant that incorporates this damping. The utility of the analytical form is demonstrated through its application to the COVID-19 pandemic.

Asymptotic approximants have been successful at creating analytical solutions to many problems in mathematical physics<sup>1-8</sup>. Like the well-known Padé approximant<sup>9,10</sup>, they are constructed to match a primary series expansion in a given region up to any specified order. Unlike Padés, however, the form of an asymptotic approximant is not limited to a ratio of polynomials, and its structure is chosen to enforce the asymptotic equivalence in a region away from the primary series expansion. By increasing the number of terms in an asymptotic approximant, it converges to the exact solution in these two regions - as well as at all points in between. Convergence is certainly a necessary condition for a valid approximant; although there is yet no proof, we find that a convergent approximant matches, with high accuracy, the numerical solutions of the governing equation systems examined thus far<sup>1-8</sup>.

The COVID-19 outbreak motivates the need to extend the application of asymptotic approximants to epidemiology models. The method has seen recent success in providing a closed-form solution to the Susceptible-Infected-Recovered (SIR) model<sup>8</sup>. Here, we extend the method to the commonly used Susceptible-Exposed-Infected-Recovered (SEIR) model. This model is formulated as a system of nonlinear ordinary differential equations, for which no exact analytic solution has yet been found. The analytic nature of the asymptotic approximant derived in what follows is advantageous, in that the accuracy and computational expense is not affected by the duration of the epidemic prediction; the form is built such that it is accurate in  $t \in [0, \infty)$  and all points in between. Depending on the duration, it may be beneficial to replace a numerical solution with the approximant within a fitting algorithm that extracts SEIR parameters. En route to the approximant, we also present an alternative formulation of the SEIR model as a single 2<sup>nd</sup>-order nonlinear differential equation in  $\ln S$ . This form enables an efficient series solution about  $t = 0$ , expansion about  $t \rightarrow \infty$ , and may itself prove to be an attractive form of

the model to enable future analysis.

The SEIR epidemic model considers the time-evolution of a susceptible population,  $S(t)$ , interacting with an exposed population,  $E(t)$ , and infected population,  $I(t)$ , where  $t$  is time. This model is expressed as<sup>11</sup>

$$\frac{dS}{dt} = -\beta SI \quad (1a)$$

$$\frac{dE}{dt} = \beta SI - \alpha E \quad (1b)$$

$$\frac{dI}{dt} = \alpha E - \gamma I, \quad (1c)$$

with a removed population (recovered + deaths),  $R(t)$ , evolved by

$$\frac{dR}{dt} = \gamma I \quad (1d)$$

and constraints

$$S = S_0, E = E_0, I = I_0, R = R_0 \text{ at } t = 0, \quad (1e)$$

where  $\beta, \alpha, \gamma, S_0, E_0, I_0, R_0$  are non-negative constant parameters<sup>11</sup>. Along with initial conditions from (1e), the solution for  $S, E$ , and  $I$  may be first obtained from (1a) through (1c) and the solution for  $R$  subsequently extracted from (1d).

We now manipulate the system (1) into an equivalent 2<sup>nd</sup>-order equation in  $\ln S$  to simplify the analysis that follows. Equations (1a) and (1b) are added to obtain

$$\frac{dS}{dt} + \frac{dE}{dt} = -\alpha E. \quad (2)$$

Solving (1c) for  $E$  and substituting into (2) then leads to

$$\frac{d^2 I}{dt^2} + (\gamma + \alpha) \frac{dI}{dt} + \alpha \frac{dS}{dt} + \alpha \gamma I = 0. \quad (3)$$

Equation (1a) is rewritten as

$$I = -\frac{1}{\beta} \frac{d \ln S}{dt} \quad (4)$$

<sup>a)</sup>Electronic mail: nsbsma@rit.edu

and substituted into (3) to arrive at the 3<sup>rd</sup>-order equation

$$\frac{d^3 \ln S}{dt^3} + (\gamma + \alpha) \frac{d^2 \ln S}{dt^2} - \alpha\beta \frac{dS}{dt} + \alpha\gamma \frac{d \ln S}{dt} = 0. \quad (5)$$

Equation (5) may be integrated to obtain

$$\frac{d^2 \ln S}{dt^2} + (\gamma + \alpha) \frac{d \ln S}{dt} - \alpha\beta S + \alpha\gamma \ln S = C, \quad (6)$$

where the integration constant

$$C = \alpha\gamma \ln(S_0) - \alpha\beta(E_0 + I_0 + S_0) \quad (7a)$$

is obtained by evaluating the right-hand side of (6) at  $t = 0$  using (1e) and (1a)-(1c). The form of equation (6) suggests that the variable substitution  $f = \ln S$  be made, and the result is

$$\frac{d^2 f}{dt^2} + (\gamma + \alpha) \frac{df}{dt} - \alpha\beta e^f + \alpha\gamma f = C \quad (7b)$$

where, from (1e) and (4),

$$f = \ln S_0, \quad \frac{df}{dt} = -\beta I_0 \text{ at } t = 0. \quad (7c)$$

Once  $f$  is solved for in the above, the solution to the SEIR model is given by

$$S = e^f \quad (8a)$$

$$I = -\frac{1}{\beta} \frac{df}{dt} \quad (8b)$$

$$R = R_0 - \frac{\gamma}{\beta} (f - \ln S_0) \quad (8c)$$

$$E = E_0 + I_0 + S_0 + R_0 - I - S - R. \quad (8d)$$

The series solution of (7) is given by

$$f = \sum_{n=0}^{\infty} a_n t^n, \quad a_0 = \ln S_0, \quad a_1 = -\beta I_0 \quad (9a)$$

$$a_2 = [C - (\alpha + \gamma) a_1 + \alpha\beta S_0 - \alpha\gamma a_0] / 2 \quad (9b)$$

$$a_{n+2} = \frac{\alpha\beta \tilde{a}_n - (\gamma + \alpha)(n+1)a_{n+1} - \alpha\gamma a_n}{(n+2)(n+1)}, \quad n > 0 \quad (9c)$$

$$\tilde{a}_{n>0} = \frac{1}{n+1} \sum_{j=0}^n (n-j+1) a_{n-j+1} \tilde{a}_j, \quad \tilde{a}_0 = S_0. \quad (9d)$$

The result (9) is obtained by the standard procedure of inserting (9a) into (7) and finding a recursion for the coefficients by equating like-terms. It is thus necessary to

obtain the expansion of the nonlinear term  $e^f \equiv S$  in (7). To do so, we solve for the coefficients of  $S = \sum \tilde{a}_n t^n$  by applying Cauchy's product rule to the chain-rule result  $f'S = S'$  and evaluate like-terms to obtain the recursive expression given by (9d). Although the series solution given by (9) is an analytic solution to (7), it is only valid within its radius of convergence and is incapable of capturing the long-time behavior of the system. This motivates the use of an approximant to analytically continue the series beyond this radius.

The long-time asymptotic behavior of the system (7) is required to develop our asymptotic approximant, and so we proceed as follows. It has been proven in prior literature<sup>12</sup> that  $S$  approaches a limiting value,  $S_\infty$ , as  $t \rightarrow \infty$ , and this corresponds to  $I \rightarrow 0$  in the same limit. Thus,  $f$  approaches a limiting value,  $f_\infty \equiv \ln S_\infty$ , as  $t \rightarrow \infty$ . The value of  $f_\infty$  satisfies the following equation<sup>12</sup>

$$e^{f_\infty} - \frac{\gamma}{\beta} (f_\infty - \ln S_0) - E_0 - I_0 - S_0 = 0 \quad (10a)$$

in the interval

$$f_\infty \in (-\infty, \ln \gamma/\beta). \quad (10b)$$

We expand  $f$  as  $t \rightarrow \infty$  as follows:

$$f \sim f_\infty + g(t) \text{ where } g \rightarrow 0 \text{ as } t \rightarrow \infty. \quad (11)$$

Equation (11) is substituted into (7),  $e^g$  is replaced with its power series expansion, and terms of  $O(g^2)$  are neglected to achieve the following linearized equation

$$\frac{d^2 g}{dt^2} + (\gamma + \alpha) \frac{dg}{dt} + (\alpha\gamma - \alpha\beta e^{f_\infty}) g = 0. \quad (12)$$

The general solution to (12) is

$$g = \epsilon_1 e^{\lambda_1 t} + \epsilon_2 e^{\lambda_2 t} \quad (13a)$$

$$\lambda_{1,2} = \frac{1}{2} \left[ -\alpha - \gamma \pm \sqrt{(\gamma - \alpha)^2 + 4\alpha\beta e^{f_\infty}} \right] \quad (13b)$$

where  $\epsilon_1$  and  $\epsilon_2$  are unknown constants and  $\lambda_2 < \lambda_1 < 0$  since  $e^{f_\infty} < \gamma/\beta$  from (10b). Thus the long-time asymptotic behavior of  $f$  is given by

$$f \sim f_\infty + \epsilon_1 e^{\lambda_1 t}, \quad t \rightarrow \infty. \quad (14)$$

Higher order corrections to the expansion (14) may be obtained by the method of dominant balance<sup>10</sup> as a series of more rapidly damped exponentials. However, the pattern by which the corrections are asymptotically ordered is not as straightforward as that of the SIR model, provided in Barlow and Weinstein<sup>8</sup>. In that work, an asymptotic approximant is constructed as a series of exponentials that exactly mimics the long-time expansion. In the SEIR model, complications in the higher-order asymptotic behavior arise from the competition between

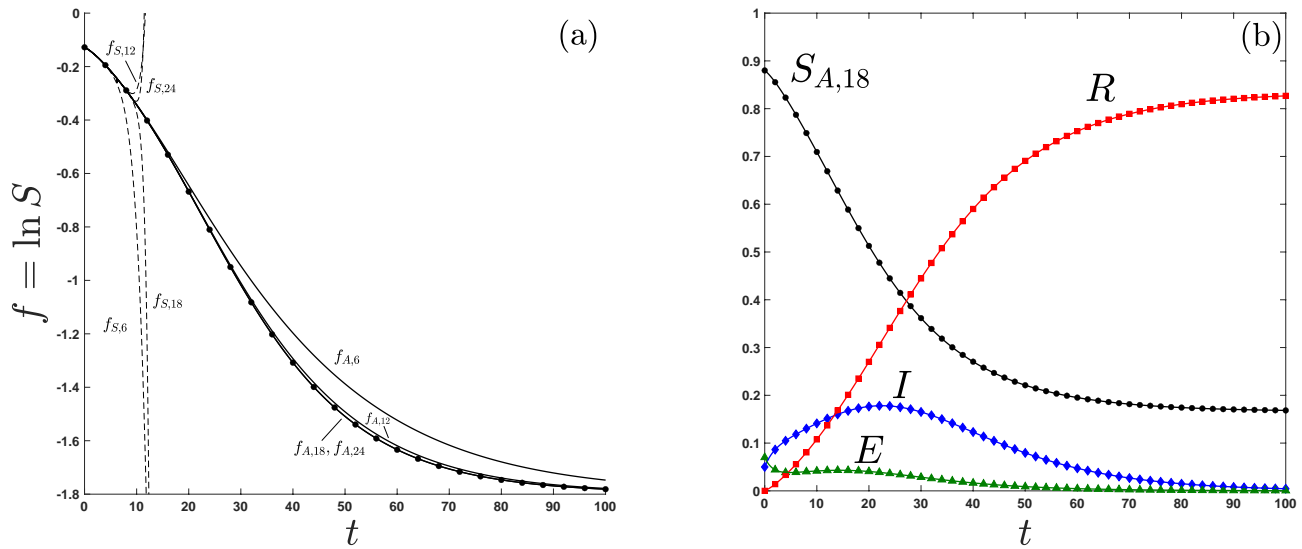


FIG. 1. Analytical and numerical solutions to the SEIR model (1), where the susceptible ( $S$ ), exposed ( $E$ ), infected ( $I$ ), and recovered ( $R$ ) populations are represented as a fraction of the total population and  $t$  is in units of days. (a) Solution shown in terms of  $f \equiv \ln S$ . As the number of terms  $N$  is increased, the series solution, denoted  $f_{S,N}$  (given by (9), dashed curves), diverges and the approximant, denoted  $f_{A,N}$  (given by (15), solid curves), converges to the exact (numerical) solution ( $\bullet$ 's). (b) The converged asymptotic approximant for  $f$  is used to obtain  $S$ ,  $E$ ,  $I$ , and  $R$  from (8) shown by solid curves and compared with the numerical solution (closed symbols). The model parameters values and initial conditions  $\alpha = 0.466089$ ,  $\beta = 0.2$ ,  $\gamma = 0.1$ ,  $S_0 = 0.88$ ,  $E_0 = 0.07$ ,  $I_0 = 0.05$ , and  $R_0 = 0$  are taken from estimates of Ebola virus propagation examined in Rachah and Torres<sup>13</sup>.

the two exponentials in (13a). Here, we enforce the leading-order  $t \rightarrow \infty$  behavior given by (14) and make a more traditional choice for matching with the  $t = 0$  expansion (9). We create an approximant with an embedded rational function with equal-order numerator and denominator (i.e., a symmetric Padé approximant<sup>10</sup>), such that it approaches the unknown constant  $\epsilon_1$  in (14) as  $t \rightarrow \infty$ , while converging to the intermediate behavior at shorter times. The assumed SEIR approximant is given by

$$f_{A,N} = f_\infty + e^{\lambda_1 t} \frac{\sum_{n=0}^{N/2} A_n t^n}{1 + \sum_{n=1}^{N/2} B_n t^n}, \quad N \text{ even} \quad (15)$$

where the  $A_n$ 's and  $B_n$ 's are obtained such that the Taylor expansion of (15) about  $t = 0$  is exactly (9). Note that, although a rational function is being used in (15), it is not a Padé approximant itself. Padés are only capable of capturing  $t^n$  behavior in the long-time limit, where  $n$  is an integer. The pre-factor  $e^{\lambda_1 t}$  is required to make (15) an *asymptotic* approximant for the SEIR model. However, we may still make use of fast Padé coefficient solvers<sup>14,15</sup> by recasting (15) as a Padé for the series that results from the Cauchy product between the expansions of  $e^{-\lambda_1 t}$  and  $f - f_\infty$ , the former which is commonly known and the latter which is given by (9) (except

with  $a_0 = \ln S_0 - f_\infty$ ). A MATLAB code for computing the  $A_n$  and  $B_n$  coefficients of (15) (given  $\alpha$ ,  $\gamma$ ,  $\beta$ ,  $S_0$ ,  $E_0$ ,  $I_0$ ) is available from the authors<sup>16</sup>.

The SEIR approximant (15) is thus an analytic expression that, by construction, matches the correct  $t \rightarrow \infty$  behavior given by (14) and whose expansion about  $t = 0$  is exact to  $N^{\text{th}}$ -order. Figure 1a provides a typical comparison of the  $N$ -term series solution (9) denoted by  $f_{S,N}$  (and dashed lines), the  $N$ -term approximant (15) denoted by  $f_{A,N}$  (solid lines), and the numerical solution ( $\bullet$ 's). Note that the series solution has a finite radius of convergence as evidenced by the poor agreement and divergence from the numerical solution at larger times, even as additional terms are included. By contrast, the approximant converges as additional terms are included. For  $N = 18$ , the approximant is visibly indistinguishable from the numerical solution (obtained by forward differencing) with a maximum relative error on the order of the numerical time-step (here  $10^{-4}$ ) over the time range indicated. Increasing the number of terms beyond  $N = 18$  does improve accuracy up to a point, but deficient approximants are possible with increasing  $N$  due to zeroes that can arise in the denominator of (15). Such approximants are ignored in assessing convergence. To avoid this behavior, the lowest number of terms that yields the desired accuracy should be chosen. The convergence of the approximant with increasing  $N$  is a necessary condition for a valid approximant. In figure 1b, the converged ( $N = 18$ ) asymptotic approximant for  $f$  is used to obtain

analytic solutions for  $S$ ,  $E$ ,  $I$ , and  $R$  from (8), which are compared with the numerical solution for these quantities. Note, that the derivative of  $f$  used in the computation of  $I$  and  $E$  is a more sensitive measure of convergence than  $f$  itself, and the approximant for  $N = 18$  provides excellent agreement between these quantities and numerics within the visible scale of the plot.

The figure 1 results described above correspond to a case examined in Rachah and Torres<sup>13</sup> to model an Ebola outbreak. In figures 2, 3, and 4, the approximant is applied to COVID-19 data<sup>17</sup> for Yunan (China), Japan, and Sweden, respectively. An increased number of terms in the approximant is required to achieve the same relative errors in each successive figure. Note that we extensively surveyed the available COVID-19 data, and the results in figures 2-4 are representative of the fits and variability in the number of terms needed to assure convergence of the approximant.

Note that the reported COVID-19 outbreak data<sup>17</sup> is provided in terms of *confirmed* cases, *recovered* individuals, and *deaths* per day. We use *recovered* + *deaths* as an approximation for the removed population  $R$  and use *confirmed* - *recovered* - *deaths* as an approximation to compare with the quantity  $I$  of the SEIR model. It is acknowledged that the actual COVID-19 data is influenced by effects not included in the SEIR model, and this can affect the ability of the model to closely fit actual COVID data. The data approximations made here are to enable comparisons with model predictions. The ability of the approximant to match numerical results is unaffected by such approximations. Disagreement between the model and epidemic data after fitting are attributed to the applicability of the SEIR model and not the approximant.

In figures 2-4, a least squares fit to  $I$  and  $R$  data is used to extract SEIR parameters  $\alpha$ ,  $\beta$ ,  $\gamma$  and initial conditions  $S_0$  and  $E_0$ . To do so, the initial values of  $I_0$  and  $R_0$  are taken directly from the COVID data set<sup>17</sup>. Additionally, the time  $t = 0$  is chosen such that disease has progressed to a point where initial trends are observed, so that curve shapes are consistent with those reasonably predicted by the SEIR model. Adjustments such as this have been well described in fits done in previous work<sup>18,19</sup>. The

initial guesses for the iterative least-squares fit are taken from data fits for earlier times than examined here<sup>18,19</sup>.

Our results demonstrate that an asymptotic approximant can be used to provide accurate analytic solutions to the SEIR model. Future work should examine the ability of the asymptotic approximant technique to yield closed-form solutions for even more sophisticated epidemic models, as well as their endemic counterparts<sup>12</sup>.

<sup>1</sup>N. S. Barlow, A. J. Schultz, S. J. Weinstein, and D. A. Kofke, *J. Chem. Phys.* **137**, 204102 (2012).

<sup>2</sup>N. S. Barlow, A. J. Schultz, S. J. Weinstein, and D. A. Kofke, *AIChE J.* **60**, 3336 (2014).

<sup>3</sup>N. S. Barlow, A. J. Schultz, S. J. Weinstein, and D. A. Kofke, *J. Chem. Phys.* **143**, 071103:1 (2015).

<sup>4</sup>N. S. Barlow, C. R. Stanton, N. Hill, S. J. Weinstein, and A. G. Cio, *Q. J. Mech. Appl. Math.* **70**, 21 (2017).

<sup>5</sup>N. S. Barlow, S. J. Weinstein, and J. A. Faber, *Class. Quant. Grav.* **34**, 1 (2017).

<sup>6</sup>R. J. Beachley, M. Mistysyn, J. A. Faber, S. J. Weinstein, and N. S. Barlow, *Class. Quant. Grav.* **35**, 1 (2018).

<sup>7</sup>E. R. Belden, Z. A. Dickman, S. J. Weinstein, A. D. Archibee, E. Burroughs, and N. S. Barlow, *Q. J. Mech. Appl. Math.* **73**, 36 (2020).

<sup>8</sup>N. S. Barlow and S. J. Weinstein, *Physica D* **408**, 1 (2020).

<sup>9</sup>G. A. Baker Jr. and J. L. Gammel, *J. Math. Anal. Appl.* **2**, 21 (1961).

<sup>10</sup>C. M. Bender and S. A. Orszag, *Advanced Mathematical Methods for Scientists and Engineers I: Asymptotic Methods and Perturbation Theory* (McGraw-Hill, 1978).

<sup>11</sup>W. O. Kermack and A. G. McKendrick, *Proc. Roy. Soc. London A* **115**, 700 (1927).

<sup>12</sup>H. W. Hethcote, in *Mathematical Understanding of Infectious Disease Dynamics*, edited by S. Ma and Y. Xia (World Scientific Publishing, 2008).

<sup>13</sup>A. Rachah and D. F. M. Torres, *Math Method Appl. Sci.* **40**, 6155 (2017).

<sup>14</sup><https://github.com/chebfun/chebfun/blob/master/padeapprox.m>.

<sup>15</sup>P. Gonnet, S. Güttel, and L. N. Trefethen, *SIAM Rev.* **55**, 101 (2013).

<sup>16</sup><https://www.mathworks.com/matlabcentral/fileexchange/?????-approximantcoefficientsseir>.

<sup>17</sup>John Hopkins University CSSE, "Novel coronavirus (covid-19) cases," <https://github.com/CSSEGISandData/COVID-19>.

<sup>18</sup>M. Peirlinck, K. Linka, F. S. Costabal, and E. Kuhl, *Biomech. Model. Mechan.* [doi.org/10.1007/s10237-020-01332-5](https://doi.org/10.1007/s10237-020-01332-5), 1 (2020).

<sup>19</sup>K. Linka, M. Peirlinck, F. S. Costabal, and E. Kuhl, *Comput. Method Biomec.* [doi.org/10.1080/10255842.2020.1759560](https://doi.org/10.1080/10255842.2020.1759560), 1 (2020).

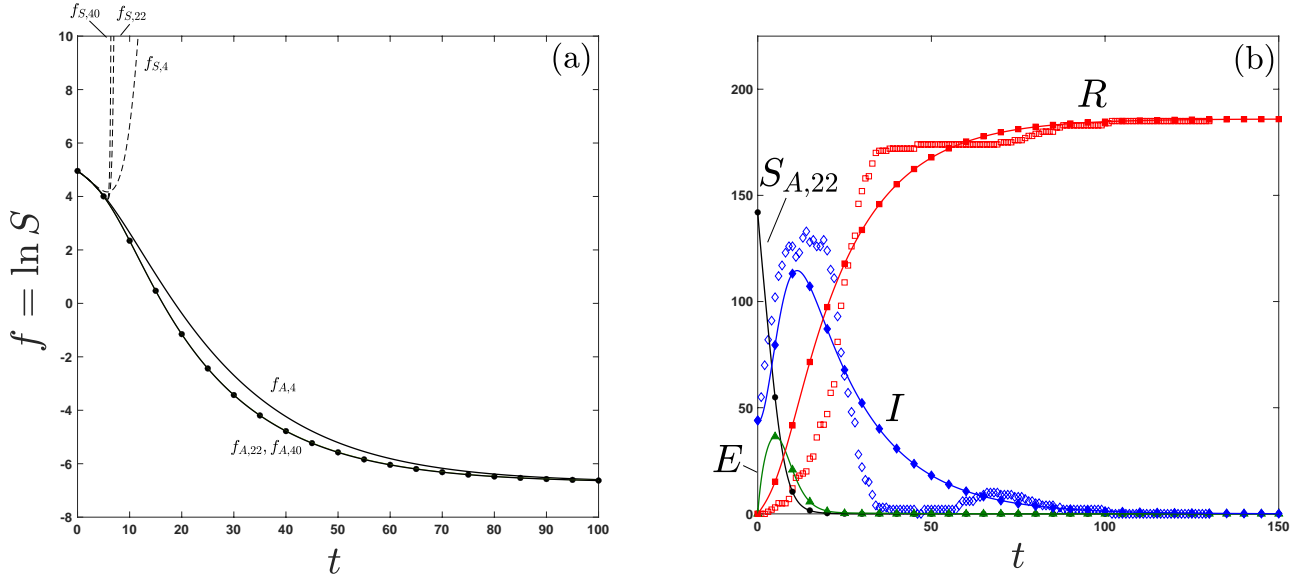


FIG. 2. Analytical and numerical solutions to the SEIR model (1), where  $S$ ,  $E$ ,  $I$ ,  $R$  are in units of people and  $t$  is in days. All other notation and labels are the same as in figure 1, except  $R$  now also includes deaths. SEIR model parameters values and unknown initial conditions are obtained via a least-squares fit to the Yunan, China COVID-19 outbreak data<sup>17</sup> (open symbols). Best fit parameters are  $\alpha=0.395031$ ,  $\beta=0.00333$ ,  $\gamma=0.0553093$ ,  $S_0=142$ , and  $E_0=0$ . The initial conditions  $I_0 = 44$  and  $R_0=0$  are taken directly from the data set<sup>17</sup> at a chosen  $t = 0$  (here January 28, 2020).

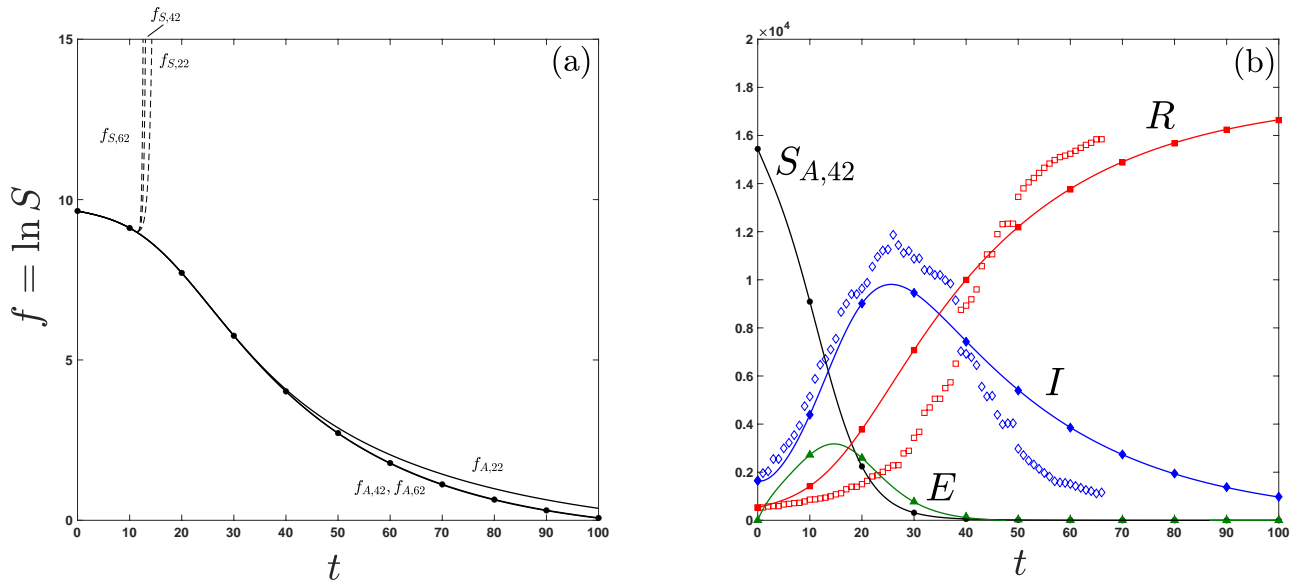


FIG. 3. Analytical and numerical solutions to the SEIR model (1), where  $S$ ,  $E$ ,  $I$ ,  $R$  are in units of people and  $t$  is in days. All other notation and labels are the same as in figure 1, except  $R$  now also includes deaths. SEIR model parameters values and unknown initial conditions are obtained via a least-squares fit to the Japan COVID-19 outbreak data<sup>17</sup> (open symbols). Best fit parameters are  $\alpha=0.2332207$ ,  $\beta=2.040015 \times 10^{-5}$ ,  $\gamma=0.034334$ ,  $S_0=15442$ , and  $E_0=0$ . The initial conditions  $I_0 = 1649$  and  $R_0=529$  are taken directly from the data set<sup>17</sup> at a chosen  $t = 0$  (here April 1, 2020).

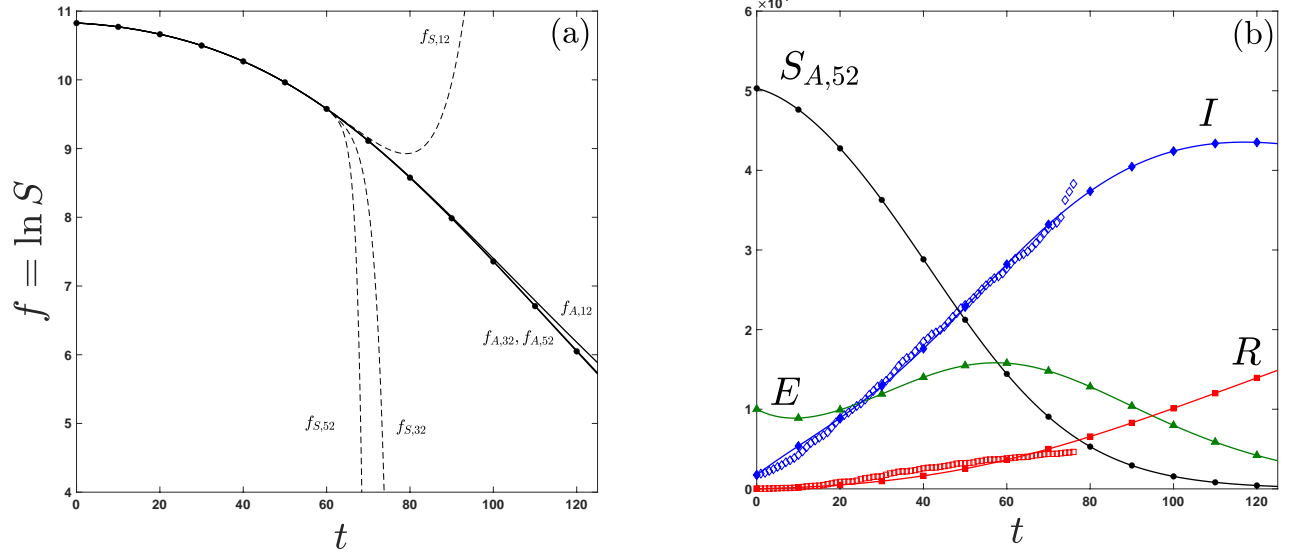


FIG. 4. Analytical and numerical solutions to the SEIR model (1), where  $S, E, I, R$  are in units of people and  $t$  is in days. All other notation and labels are the same as in figure 1, except  $R$  now also includes deaths. SEIR model parameters values and unknown initial conditions are obtained via a least-squares fit to the Sweden COVID-19 outbreak data<sup>17</sup> (open symbols). Best fit parameters are  $\alpha=0.041281$ ,  $\beta=1.513332 \times 10^{-6}$ ,  $\gamma=0.004407$ ,  $S_0=50306$ , and  $E_0=10015$ . The initial conditions  $I_0 = 1743$  and  $R_0=20$  are taken directly from the data set<sup>17</sup> at a chosen  $t = 0$  (here March 22, 2020).